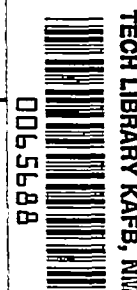


8799 6678
NACA TN 2399



NATIONAL ADVISORY COMMITTEE FOR AERONAUTICS

TECHNICAL NOTE 2399

APPLICABILITY OF THE HYPERSONIC SIMILARITY RULE TO PRESSURE
DISTRIBUTIONS WHICH INCLUDE THE EFFECTS OF ROTATION
FOR BODIES OF REVOLUTION AT ZERO ANGLE OF ATTACK

By Vernon J. Rossow

Ames Aeronautical Laboratory
Moffett Field, Calif.



Washington

June 1951

TECHNICAL NOTE

AD-2399

IV

319.90/41

PERMANENT



NATIONAL ADVISORY COMMITTEE FOR AERONAUTICS

TECHNICAL NOTE 2399

APPLICABILITY OF THE HYPERSONIC SIMILARITY RULE TO PRESSURE
DISTRIBUTIONS WHICH INCLUDE THE EFFECTS OF ROTATION
FOR BODIES OF REVOLUTION AT ZERO ANGLE OF ATTACK

By Vernon J. Rossow

SUMMARY

The analysis of Technical Note 2250, 1950, is extended to include the effects of flow rotation. It is found that the theoretical pressure distributions over ogive cylinders can be related by the hypersonic similarity rule with sufficient accuracy for most engineering purposes.

The error introduced into pressure distributions and drag of ogive cylinders by ignoring the rotation term in the characteristic equations is investigated. It is found that the influence of the rotation term on pressure distribution and drag depends only upon the similarity parameter K (Mach number divided by fineness ratio). Although the error in drag, due to neglect of the rotation term, is negligible at $K=0.5$, the error is about 30 percent at $K=2.0$.

Charts are presented for the rapid determination of pressure distributions for rotational flow over ogive cylinders for all values of the similarity parameter between 0.5 and 2.0 within given defined limits of Mach number and fineness ratio.

INTRODUCTION

The hypersonic similarity rule for irrotational flow over bodies of revolution at zero angle of attack was developed by Tsien and reported in reference 1. This rule states that, for hypersonic flow about geometrically similar bodies of different fineness ratio, the pressure distribution depends only on the similarity parameter K , which is the ratio of Mach number to fineness ratio. This means that, if the pressure distribution or drag is known for a given body, the pressure distribution or drag is also known for all similarly shaped bodies having the same value of the similarity parameter.

The hypersonic similarity rule, as originally developed, was restricted to irrotational flow around slender bodies at Mach numbers

PERMANENT
RECEIVED

much greater than 1. The slender body and Mach number limitation were investigated in reference 2 by comparing theoretical pressure distributions over cones and ogive cylinders. The hypersonic similarity rule was found to be applicable to bodies of revolution over a much greater range of Mach numbers and fineness ratios than would be expected from the limitations in the development.

The question of hypersonic similarity in rotational flow was considered by Hayes in reference 3. He concluded that the hypersonic similarity rule should be applicable for rotational as well as irrotational flow. However, the exactness of the similarity and the range of conditions over which it applies have apparently not been investigated for rotational flow.

The theoretical pressure distributions of reference 2 were obtained by the method of characteristics. In applying the characteristic equations the shock wave was allowed to curve, but the resulting entropy gradient or rotation was ignored by not including the rotation term in the characteristic equations.¹ This is a method commonly employed in applying the method of characteristics.

It is the primary purpose of this report to extend the examination of reference 2 to determine the degree of applicability of the hypersonic similarity rule when the rotation term in the characteristic equations is included in the computations.

A second purpose is to investigate the error introduced into the pressure distributions over ogive cylinders by ignoring the rotation term in the computations. The influence of the rotation term in the characteristic equations will hereafter be referred to as rotation or the effect of rotation.

SYMBOLS

C_D drag coefficient² $\left(\frac{\text{drag}}{q_0 S_b} \right)$

c_p specific heat of the gas at constant pressure

¹Although this type of solution is often referred to as being irrotational, it is not in the strict sense. The flow field is rotational since the shock wave is allowed to curve, but the resulting entropy gradient is ignored in the integration of the flow field.

²In this report C_D refers only to that part of the drag contributed by the pressure acting on the body nose. The nose of the body is considered to include the section forward of the cylindrical section or forward of maximum diameter.

- c_v specific heat of the gas at constant volume
- d maximum diameter of body
- df^* velocity projection along right characteristic in hodograph plane referred to critical velocity
- dg^* velocity projection along left characteristic in hodograph plane referred to critical velocity
- H total pressure
- K similarity parameter $\left(\frac{M_0}{l/d} \right)$
- l length of nose of body
- l/d fineness ratio of nose of body
- M Mach number
- M^* ratio of local speed to critical speed of sound $\left[\frac{\gamma + 1}{(\gamma - 1) + (2/M^2)} \right]^{\frac{1}{2}}$
- p static pressure
- q dynamic pressure
- R perfect gas constant
- s entropy
- S_b maximum cross-sectional area of body
- x longitudinal coordinate of body measured from vertex
- y coordinate perpendicular to body axis of symmetry
- α Mach angle
- θ local angle of inclination of streamline measured relative to the body axis
- γ ratio of specific heats of the gas $\left(\frac{c_p}{c_v} \right)$
- ϕ angle of inclination of shock wave measured relative to the body axis

Subscripts

- i conditions wherein rotation term is ignored in the characteristic equations
- o free-stream conditions
- r conditions wherein rotation term is included in the characteristic equations

SCOPE OF INVESTIGATION

The present investigation was planned to parallel that of reference 2, in which ogive cylinders³ and cone cylinders were studied. However, as illustrated in figure 1, the head pressure drag of cone cylinders is not affected by rotation. Therefore, the cone cylinders were not included in the present investigation.

In order to make use of and allow comparison with the solutions of reference 2, ogive fineness ratios and Mach numbers were selected according to the following schedule:

$\frac{K}{}$	$\frac{M}{}$	$\frac{l/d}{}$
0.5	3	6
	6	12
1.0	3	3
	6	6
	9	9
1.5	6	4
2.0	6	3
	12	6

This range was originally chosen in such a way that the similarity rule could be checked at several values of the similarity parameter K .

³The ogive referred to in this report is one-half the body of revolution formed by revolving a segment of a circle about its chord line. The cylinder is tangent to the ogive at its maximum radius.

PROCEDURE

The applicability of the hypersonic similarity rule to rotational flows was investigated by comparing theoretical pressure distributions (method of characteristics) over ogive cylinders of different fineness ratios at a fixed value of the similarity parameter K . In an effort to avoid the imposing task of obtaining the complete characteristic solutions, a means was sought of correcting the existing characteristic solutions of reference 2 which ignored the effect of rotation. An approximate method of doing this was developed and is presented in the appendix. The method permits the effect of the rotation term in the characteristic equations to be computed independently and added to the incomplete solution for the velocity distribution over the body. Once the incomplete solution is available, the time required to obtain the approximate correction for the effects of rotation is about 5 or 6 hours per solution.

Certain assumptions which conceivably could result in serious error were made in the development of the approximate method. To evaluate the magnitude of these errors, a complete solution to the characteristic equations including the rotation term was made in a case where the effects of rotation are pronounced and is compared with the corresponding approximate solution in figure 2. A curve is faired through the points computed by the characteristic solution. The points computed by the approximate method fall very close to the faired curve — the scatter or deviation lying within the accuracy of a characteristic solution. This indicates that the assumptions made in developing the approximate method do not introduce large errors. A more detailed picture of why it is possible to make the approximations and still obtain satisfactory results is given in the appendix. It is concluded that the corrected solutions are accurate enough for the present investigation.

To employ the method of characteristics, the flow conditions must be known along some curve in the flow field. The velocity and stream direction for the complete characteristic solution presented in figure 2 were obtained by approximating the ogive nose tip with a cone tangent at 5 percent of the nose length. The entropy variation was taken from a characteristic solution started at $1\frac{2}{3}$ percent of the nose length. Along the body streamline the entropy was that resulting from a shock wave due to the vertex angle of the true ogive. This same shock wave strength was used in computing total head loss and pressure distribution. The pressure coefficient at the nose vertex of the ogive was obtained by graphical interpolation of Kopal's tables (reference 4) for a cone angle equal to the true vertex angle of the ogive. Procedure IIIA of reference 5, which includes the rotation effect, was used to evaluate conditions in the flow field once the starting conditions were established.

RESULTS AND DISCUSSION

Evaluation of the Hypersonic Similarity Rule for Rotational Flow

The pressure distributions over ogive cylinders, obtained by the approximate method for rotational flow mentioned in the previous section, are shown in figure 3 for several values of the similarity parameter K . For each value of K a mean curve is faired through the computed points for all solutions. The points of each solution fall very close to the mean faired curve, both on the ogive and on the cylinder. From these results, it is evident that the hypersonic similarity rule applies for the actual rotational flow as it did for the solutions presented in reference 2. Hence, the pressure distributions with rotation effects included are a function of the similarity parameter K only. Although specifically proven for the ogive cylinder only, this conclusion would be expected to apply to other pointed bodies of revolution.

Range of Applicability of the Similarity Rule

It is of value to determine the limiting Mach numbers and fineness ratios beyond which the hypersonic similarity rule does not apply. Reference 2 presents a detailed discussion of a method by which the range of applicability of the hypersonic similarity rule can be analyzed for any pointed body. This method gives the range of similarity in pressure at the nose vertex only. It was demonstrated that deviations from similarity on the remainder of the body would not be greater than at the nose vertex.

The method of reference 2 may be used to determine the range of similarity when the effects of rotation are included, provided that deviations from similarity on the body are still nowhere greater than at the nose vertex. As in reference 2, this was investigated by using test solutions. The three test solutions of reference 2 were corrected for rotation and are compared in figure 4 with the solutions of figure 3. These solutions indicate that when rotation is included the nose vertex is still a critical point for similarity. Since the nose vertex pressure is not altered by rotation, the range of similarity for ogives is the same as shown in figure 4(b) of reference 2 and reproduced in figure 5 of this report.

Although not specifically proven here, it would be expected that the nose vertex would serve as a test for the range of similarity for pointed bodies having their maximum slope at the nose vertex.

Effect of Rotation Term on Pressure Distribution and Drag Parameter for Ogives

The dotted curve shown in figure 3 was computed by Sauer's graphical method of characteristics. This method is one commonly used in applying the method of characteristics. The shock wave is allowed to curve, but the resulting entropy gradient is ignored. The solid curves shown in figure 3 are the solutions obtained by the method of this report and include the effects of this entropy gradient.⁴

The difference between these two curves represents the error in pressure which results if the entropy term in the characteristic equations is ignored. This difference will be referred to as the effect of rotation. This difference is a function of both the longitudinal coordinate and the similarity parameter K . However, at a given station on the ogive cylinder the pressure rise due to including the rotation term is a function of K only. This fact is borne out in figure 6(a) where this pressure rise is plotted as a function of the longitudinal coordinate for various values of K . The points shown for each value of K fall very close to the faired curve. From this figure, it is apparent that the effect of rotation changes very rapidly with similarity parameter K . At $K=0.5$, the pressure increment due to rotation is negligible; whereas, at $K=2.0$, it reaches over 11 percent of the nose tip pressure. This rapid change in magnitude of the rotation effect is shown in figure 6(b) for several values of the longitudinal coordinate. These curves demonstrate that the error introduced by ignoring the entropy term in the characteristic equations can markedly affect pressure distributions determined by the method of characteristics.

Since the pressure distribution over ogives is influenced by rotation, the drag parameter C_{Dq_0}/p_0 is also influenced. The pressure distributions shown in figure 3 were integrated for drag. These drag parameters are compared in figure 7 with the ogive drag parameters of figure 11 of reference 2. The error in drag due to neglecting rotation is negligible at $K=0.5$, but amounts to a decrease in drag at $K=2.0$ of about 30 percent of the drag obtained when the effects of rotation are included. This clearly shows that in certain cases the effects of rotation can be sizable.

⁴A third type of solution which has a fictitious irrotational flow field was studied. In this case, the flow field is made completely irrotational by forcing the shock wave to remain straight. In the case studied ($l/d=3$ ogive at $M_0=6$), the resulting pressure distribution fell between the pressure distributions with rotation effects considered and ignored, being nearer the solution ignoring rotation.

Rapid Method for Determining Pressure Distributions Over Ogive Cylinders

Since the pressure distributions over ogive cylinders have been shown to be a function of K only, it is possible to plot the pressure coefficient at a given station as a function of the similarity parameter K . This should then enable the interpolation for pressure distributions at intermediate values of K . Such a graph was included in reference 1 for the solutions obtained with rotation ignored. A new graph, the values for which include the effects of rotation, has been prepared and is presented in figure 8. Thus, if M_0 and l/d are known, K is fixed and the pressure coefficient⁵ $p-p_0/p_0$ for various stations can be read directly. Since the pressures obtained when the rotation term was ignored are low by an appreciable amount at the higher values of K , figure 8 should be used in preference to figure 6 of reference 2. Over the range indicated in figure 5, pressure distributions obtained from figure 8 are believed to be accurate within a few percent which should be sufficient for most uses.

Effect of Rotation Term on Drag of Other Body Shapes

Rotation has so far been considered over two body shapes, the cone cylinder and the ogive cylinder. By considering the fundamental nature of the rotation effect, certain conclusions can be reached as to its importance on other shapes.

Rotation enters the computations when an entropy gradient exists normal to the streamlines (reference 5). The stronger the entropy gradient, the greater will be the rotation in the flow field. An entropy gradient results when a shock wave is curved in a uniform stream. This is shown by the basic supersonic equation for total head ratio across a shock wave:

$$\frac{-\Delta s}{R} = F(M_0 \sin \phi) = \left[\frac{(\gamma+1)M_0^2 \sin^2 \phi}{(\gamma-1)M_0^2 \sin^2 \phi + 2} \right]^{\frac{\gamma}{\gamma-1}} \left[\frac{\gamma+1}{2\gamma M_0^2 \sin^2 \phi - (\gamma-1)} \right]^{\frac{1}{\gamma-1}} = \frac{H}{H_0}$$

which shows that for a given body in a uniform free stream the shock wave angle ϕ must change to produce an entropy gradient.

⁵The more common pressure coefficient $p-p_0/q_0$ can be readily obtained by the relation:

$$\frac{p-p_0}{q_0} = \frac{p-p_0}{p_0} \frac{p_0}{q_0} = \frac{p-p_0}{p_0} \frac{2}{\gamma M_0^2}$$

The cases where the effect of rotation on pressure drag can be neglected are divided into two groups. The first group consists of instances where the maximum total head loss or entropy change through the head shock wave is small. It is then impossible to have an entropy gradient of any magnitude and so rotation effects will be negligible. This situation arises when the free-stream Mach number is near 1 or in the case of a very slender body at Mach numbers greater than 1. The ogive solutions shown in figure 3(a) are examples of the latter. In figure 9, the percentage change in the drag of ogives due to ignoring rotation is plotted as a function of total head loss through the nose tip shock wave. This figure indicates that if the error is restricted to 5 percent, rotation effects can be ignored only in the case of very weak shock waves.

The second group consists of those body shapes for which, regardless of the total head loss across the head shock wave, rotation will not influence the pressure drag. This will be the case for bodies where the head shock wave does not curve until far enough out so that its curvature cannot influence the head drag. The cone and cone cylinder are examples of this (fig. 1(a)). The pressure distribution on the cylindrical part will be influenced, but head drag will remain unaffected. This emphasizes the importance of distribution of body curvature. If the body has large curvature near the nose vertex, the influence of rotation on head drag will be greater than if the curvature is in the afterportion of the body.

Blunt Nosed Body Shapes

The hypersonic similarity rule would not be expected to apply rigorously to blunt nosed bodies. This follows from an examination of the assumptions made in the development of the rule. The assumptions of slender bodies and hypersonic flow are violated by flow over blunt nosed bodies. At the nose tip section the blunt nosed bodies cannot be considered slender because the body slope is infinite. This results in a detached shock wave and a region of transonic flow rather than hypersonic flow.

Furthermore, if there is to be similarity in drag, the pressure at any station must be a function of K alone. But the pressure at the nose tip of a blunt body is the stagnation pressure and so is a function of Mach number alone and not of K alone. Likewise, the total head loss and entropy of the body streamline is a function of free-stream Mach number alone and not K alone. For this reason, the pressure

increment due to rotation effects would not be expected⁶ to be a function of K alone as was the case for ogives (fig. 6).

CONCLUDING REMARKS

The hypersonic similarity rule for bodies of revolution is applicable with the same accuracy for the solutions including rotation effects as it was for the solutions in which these effects were ignored. The range of applicability for ogives is the same as it was for the incomplete solutions. Within this range the pressure distributions over ogive cylinders (which include effects of rotation) are presented on a single graph.

The effect of omitting the rotation term in the characteristic equations is to decrease the pressure which in turn decreases the drag. The drag is decreased by varying amounts depending on the body shape and the similarity parameter K . Although the rotation effect is negligible for ogives at $K=0.5$, it accounts for about 30 percent of the drag at $K=2.0$. Hence care must be taken as to when the rotation term can or cannot be ignored.

It is emphasized that, although rigorously speaking the hypersonic similarity rule would not be expected to hold for blunt nosed bodies, deviations from similarity would probably be a matter of degree so that for very slight tip-bluntness similarity might still hold except in the vicinity of the tip.

Ames Aeronautical Laboratory,
National Advisory Committee for Aeronautics,
Moffett Field, Calif.

⁶In spite of the above considerations, it is felt that the hypersonic similarity rule would still be useful for the over-all drag of slightly blunt bodies. It is believed, however, that some limit of tip bluntness would be reached beyond which the hypersonic similarity rule would not apply.

APPENDIX

DEVELOPMENT AND PROOF OF APPROXIMATE METHOD

The approximate method for correcting for the rotation term in the characteristic equations is developed from the method of characteristics for axially symmetric flow. The characteristic equations written in Sauer's notation according to reference 5 (p. 35) for rotational and irrotational flow are:

$$\text{Left: } df_r^* = \frac{M^* \sin \theta \sin^2 \alpha d\eta}{\gamma} - \frac{M^* \sin^2 \alpha \cos \alpha d\frac{s}{R}}{\gamma} \quad (A1)$$

$$\text{Right: } dg_r^* = \frac{M^* \sin \theta \sin^2 \alpha d\xi}{\gamma} - \frac{M^* \sin^2 \alpha \cos \alpha d\frac{s}{R}}{\gamma} \quad (A2)$$

$$\text{Left: } df_i^* = \frac{M^* \sin \theta \sin^2 \alpha d\eta}{\gamma} \quad (A3)$$

$$\text{Right: } dg_i^* = \frac{M^* \sin \theta \sin^2 \alpha d\xi}{\gamma} \quad (A4)$$

The difference between the rotational and irrotational flow equations is the additional term involving entropy in the rotational equations. This additional term represents a change in velocity increment due to rotation, given by

$$\text{Left: } - \frac{1}{\cos \alpha} \frac{M^* \sin^2 \alpha \cos \alpha \Delta \frac{s}{R}}{\gamma} \quad (A5)$$

$$\text{Right: } - \frac{1}{\cos \alpha} \frac{M^* \sin^2 \alpha \cos \alpha \Delta \frac{s}{R}}{\gamma} \equiv \Delta M^* \quad (A6)$$

The $1/\cos \alpha$ is required because the complete entropy term of equations (A1) and (A2) is applied along the characteristic direction, whereas the velocity increment is applied along the stream direction.

The physical significance of equation (A6) is shown in another form of this equation. From reference 6, the velocity increment ΔM^* becomes:

$$\Delta M^* = \frac{M^* \sin^2 \alpha}{\gamma} \Delta \frac{s}{R} = \frac{2 \omega \Delta n}{a^*}$$

where

ω angular velocity of rotation of the flow field

Δn distance measured perpendicular to the streamlines from known point to new unknown point

a^* critical velocity of sound

Hence, in proceeding from a known point in the flow field to a new unknown point, ΔM^* is the product of the angular velocity of rotation and the distance, perpendicular to the streamlines, between the two points. The term ΔM^* is the contribution to the velocity, at the new point, made by the entropy gradient.

The approximate method consists of evaluating equation (A6) along the individual right-hand Mach lines between the shock wave and body in one step to obtain the increments in surface velocity due to rotation. These increments are added algebraically to the velocities determined by ignoring rotation and the resulting velocities are then used to compute a new pressure distribution. The terms M^* , α and $\Delta(s/R)$ are taken from the characteristic solutions where rotation was ignored. The term $\Delta(s/R)$ is the total entropy difference between the shock wave end and the body end of the right-hand characteristics. It is to be noted that the approximate method corrects the velocity along the surface only and is not applicable for the rest of the flow field.

Several approximations are made in applying the approximate method. It is possible to show qualitatively how the approximations enter into the solutions and why they can be made. This is done in figure 10 by comparing in the hodograph plane a complete characteristic solution with a solution by the approximate method.⁷ The points having the subscript r are computed by the method of characteristics⁸ with rotation effects included (equations (A1) and (A2)). This method is the most refined available at present and so the points 1_r through 4_r represent the desired solution. The points 1_i on the shock wave through 4_i on the body were computed by the method of characteristics ignoring the rotation term. These points differ by a sizable amount from those obtained by the more refined method, indicated by subscript r , both on the body and at the shock wave. The approximate method consists of subtracting the appropriate ΔM^* from the velocity at the body points, 2_i and 4_i . This step is shown in figure 10 and the body points so computed are 2_a and 4_a . It can be seen that 2_a and 4_a agree very closely with 2_r and 4_r .

⁷The construction is schematic and therefore not drawn to scale. All the computation dimensions have been exaggerated.

⁸For details of procedure, see reference 5, procedure IIIA.

Along the right-hand Mach line the approximate method is equivalent to the complete method of characteristics. The only difference is that ΔM^* is computed along the stream direction rather than along the characteristic direction, but this does not affect the magnitude of the velocity increment. The two methods are not, however, equivalent along the left-hand Mach line. Along this Mach line, the velocity increment due to rotation produces a difference in shock-wave strength between the solution with rotation effects included and the solution with these effects neglected. However, this difference does not strongly influence the velocity at the body. The reason for this is that the left-hand characteristic in the hodograph plane is nearly perpendicular to the shock polar which minimizes the effect of rotation introduced by equation (A5). Therefore, at the body the two solutions are nearly equivalent. The departure from perpendicularity is a measure of the magnitude of the error of the approximate method and is indicated⁷ in figure 10(a). If the shock polar had the same slope as an epicycloid,⁸ the left characteristic line would in all cases be perpendicular to the shock polar. For this case, then, there would be no error in the approximate method. The shock polar is identical with an epicycloid near the zero stream deflection and deviates a little as the stream angle increases. Therefore, it can be concluded that the approximate method is applicable to most bodies of revolution and is not restricted to ogives.

In the preceding analysis a large Mach net was considered. To investigate the errors introduced by using a large net, a solution with a large net, such as is shown in figure 10(b), was compared with a small net solution. The two solutions agreed identically at the shock wave and at the body. The large net solution was obtained using mean value procedure as were all other solutions, but required more reiterations before converging to the single point in the hodograph plane.

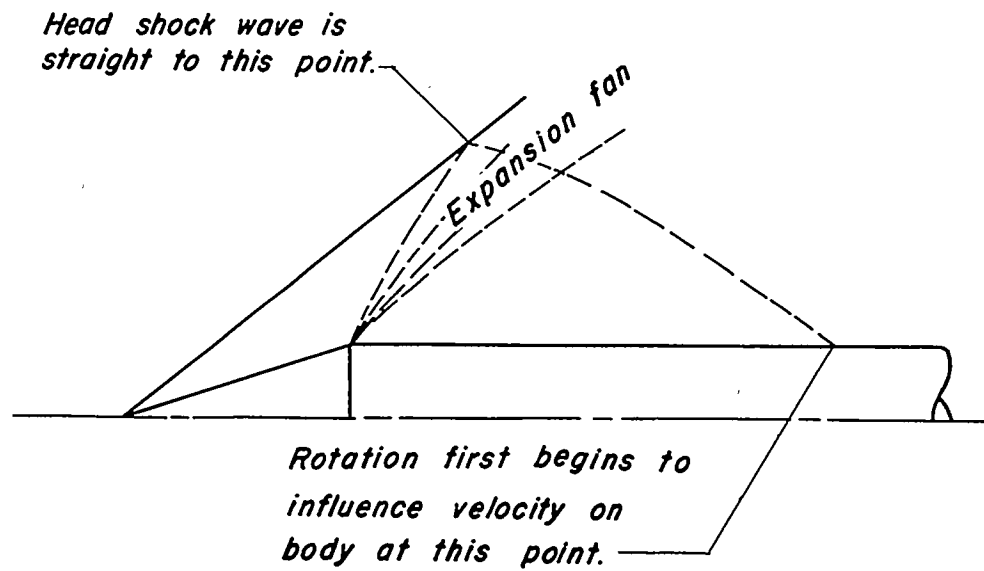
An estimate of the over-all error introduced by the various approximations was obtained by comparing an approximate solution with a conventional characteristic solution with rotation effects included in a case where these effects are large. Two such solutions are compared in figure 2 for a fineness ratio 3.0 ogive at a free-stream Mach number of 6.0 — similarity parameter K of 2.0. As was pointed out in the body of the report, the two solutions agreed within the accuracy of a characteristic solution.

⁷See footnote, page 12.

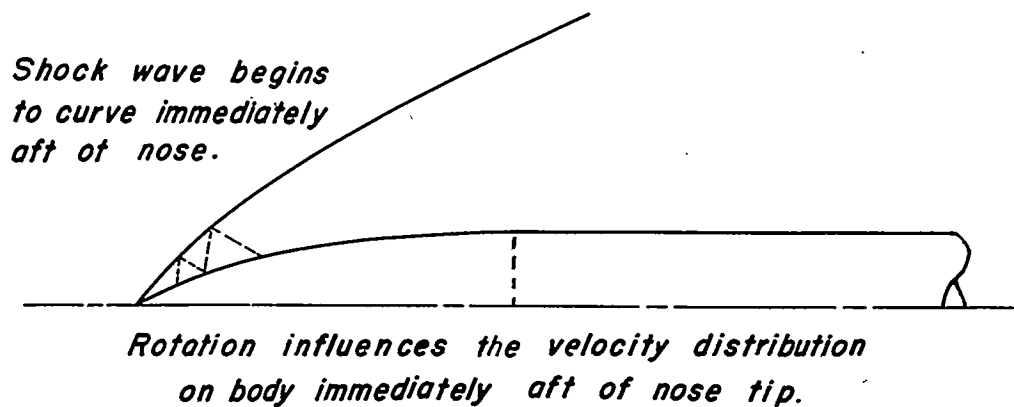
⁸An epicycloid is the locus of the velocity vector for two-dimensional isentropic expansion.

REFERENCES

1. Tsien, Hsue-Shen: Similarity Laws of Hypersonic Flows. Jour. Math. and Phys., vol. 25, no. 3, Oct. 1946.
2. Ehret, Dorris M., Rossow, Vernon J., and Stevens, Victor I.: An Analysis of the Applicability of the Hypersonic Similarity Law to the Study of Flow About Bodies of Revolution at Zero Angle of Attack. NACA TN 2250, 1950.
3. Hayes, Wallace D.: On Hypersonic Similitude. Quarterly of Applied Mathematics, vol. V, no. 1, Apr. 1947.
4. Massachusetts Institute of Technology, Dept. of Electrical Engineering, Center of Analysis: Tables of Supersonic Flow Around Cones, by the Staff of the Computing Section, Center of Analysis, under the direction of Zdenek Kopal. Tech. Rep. No. 1, Cambridge, 1947.
5. Isenberg, J. S.: The Method of Characteristics in Compressible Flow. Part I (Steady Supersonic Flow) Tech. Rep. F-TR-1173A-ND, USAF, Air Materiel Command, Wright Field, Technical Intelligence (Brown University, Graduate Division of Applied Mathematics, A-9-M II/1), Dec. 1947.
6. Liepmann, H. W., and Lapin, Ellis: Summary of Characteristics Methods for Steady State Supersonic Flows. Douglas Aircraft Company Inc., Rep. SM-13343, Mar. 3, 1949.



(a) Cone.



(b) Ogive.



Figure 1.—Schematic diagram showing where rotation begins to influence the velocity distribution on cone cylinders and ogive cylinders.

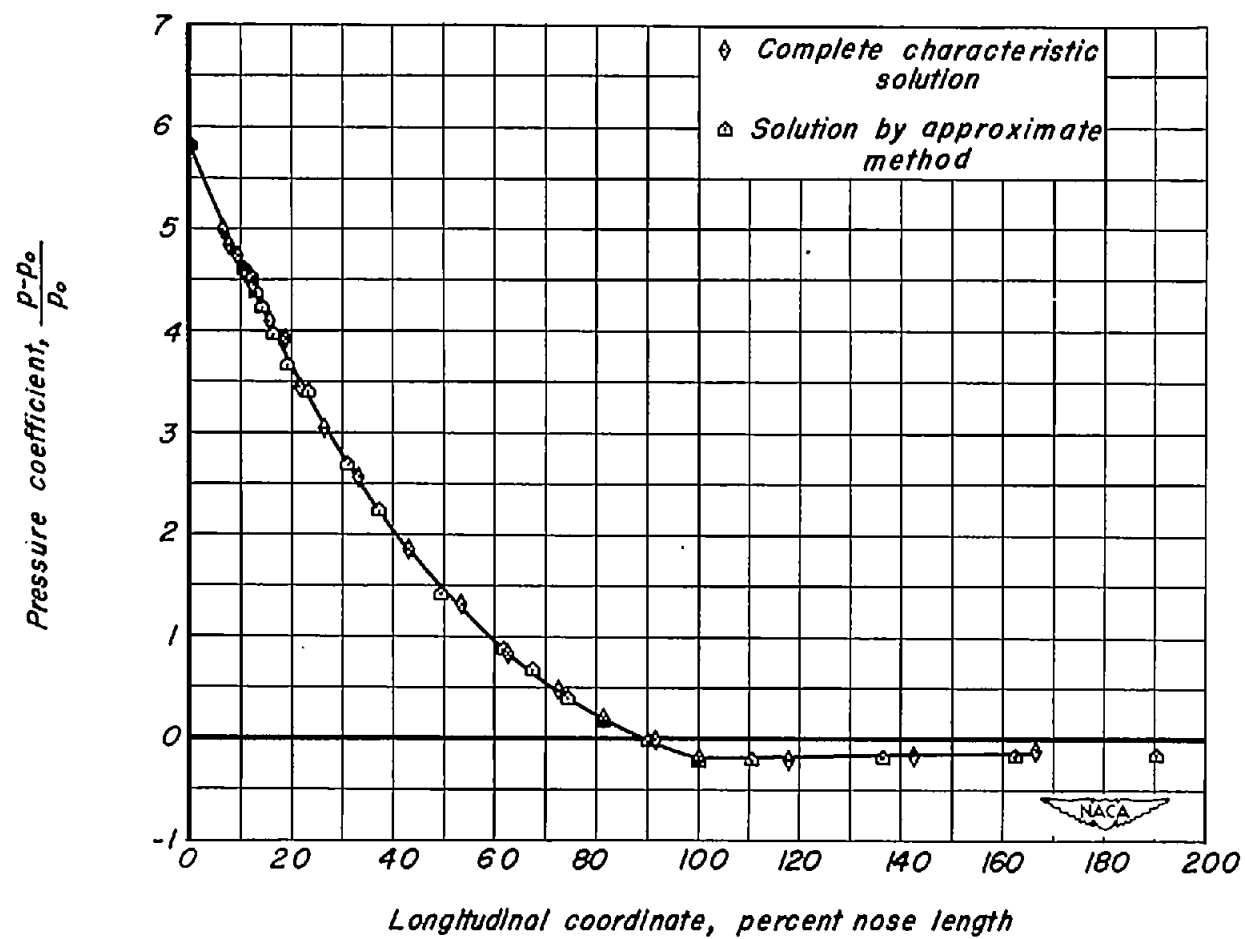
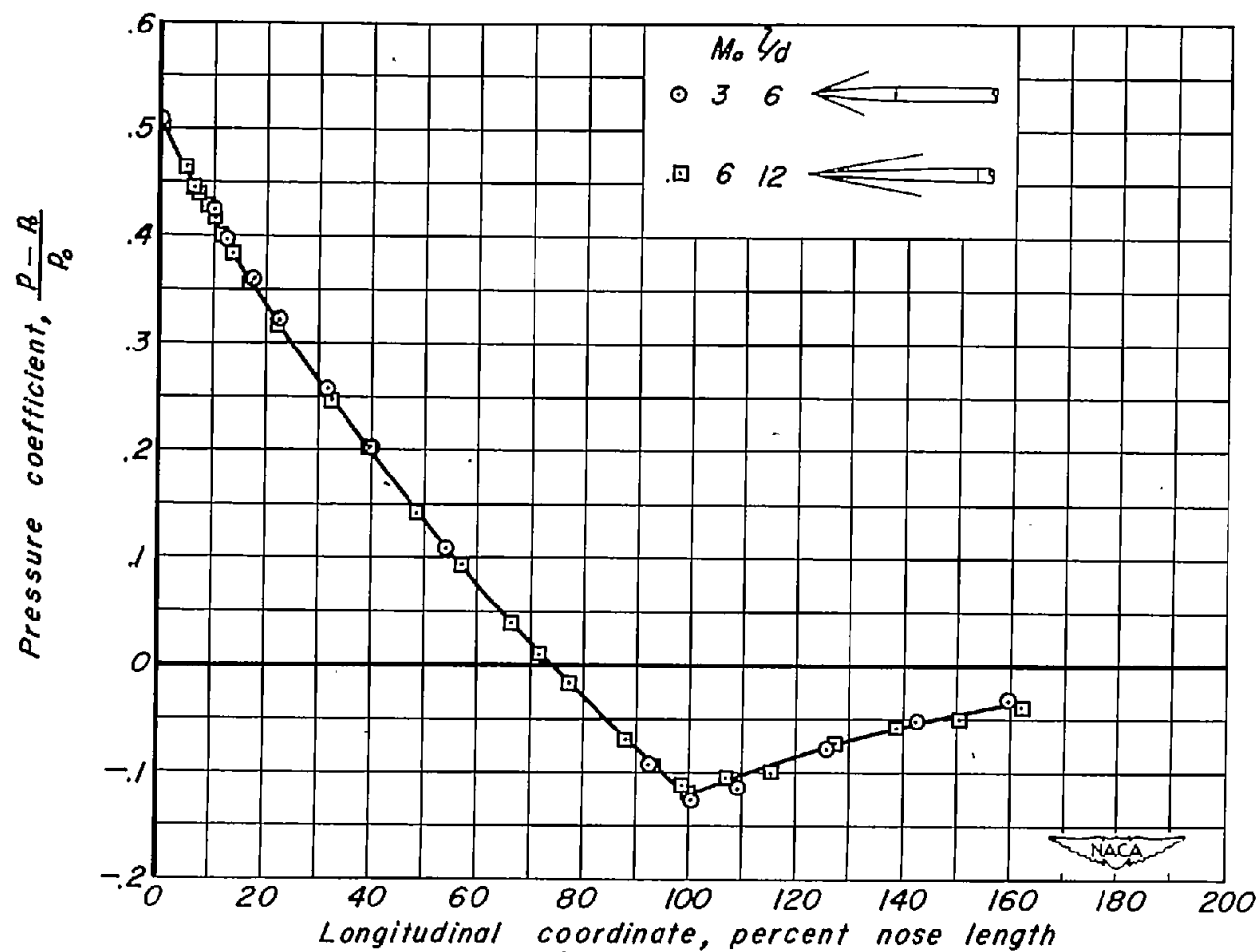


Figure 2.—Comparison of a solution by the approximate method with a complete characteristic solution;
 $K=2$, $l/d=3$, $M=6$.



(a) $K = 0.5$

Figure 3.—Variation of pressure coefficient along ogive cylinders for a given value of the similarity parameter K .

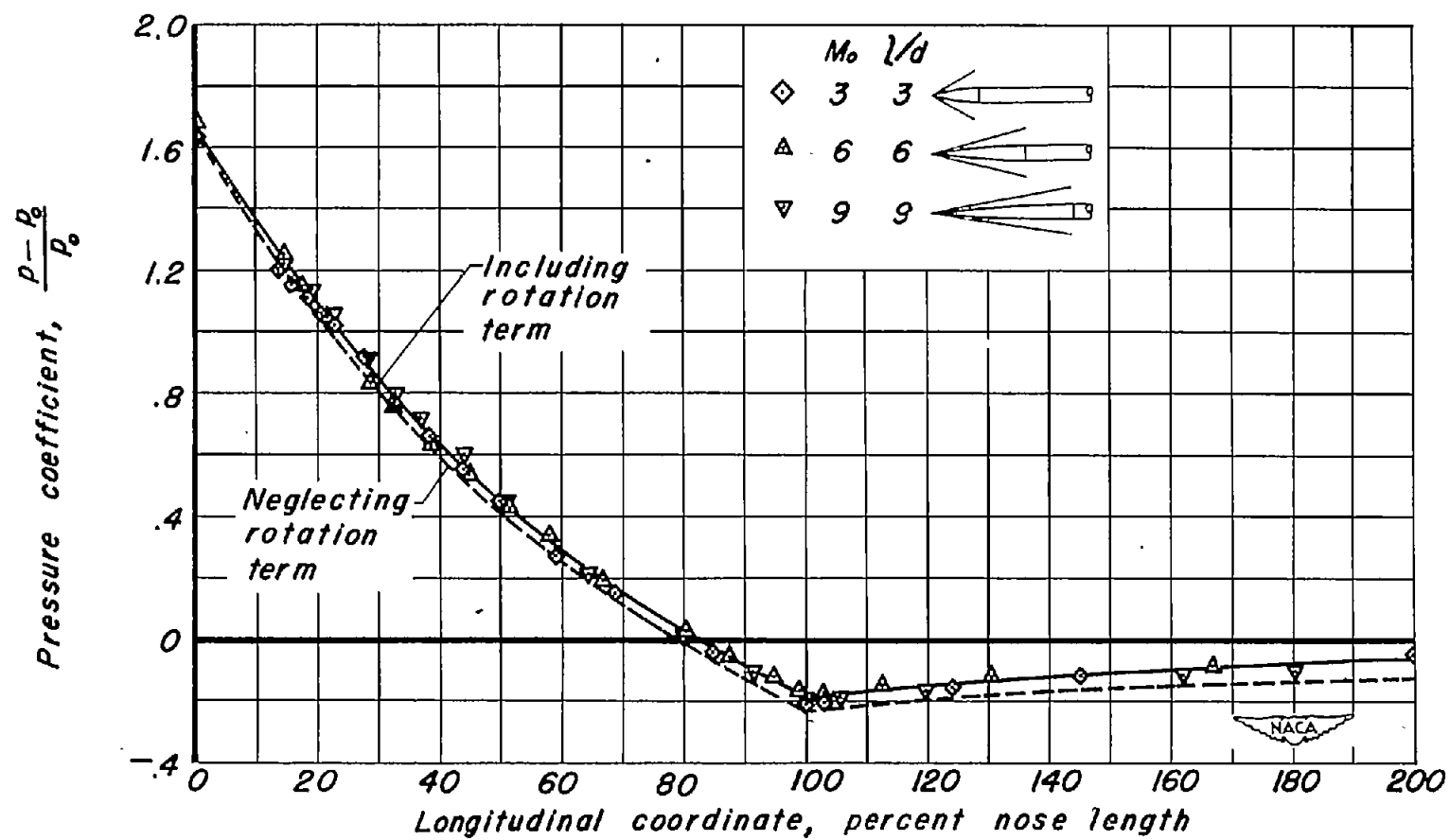
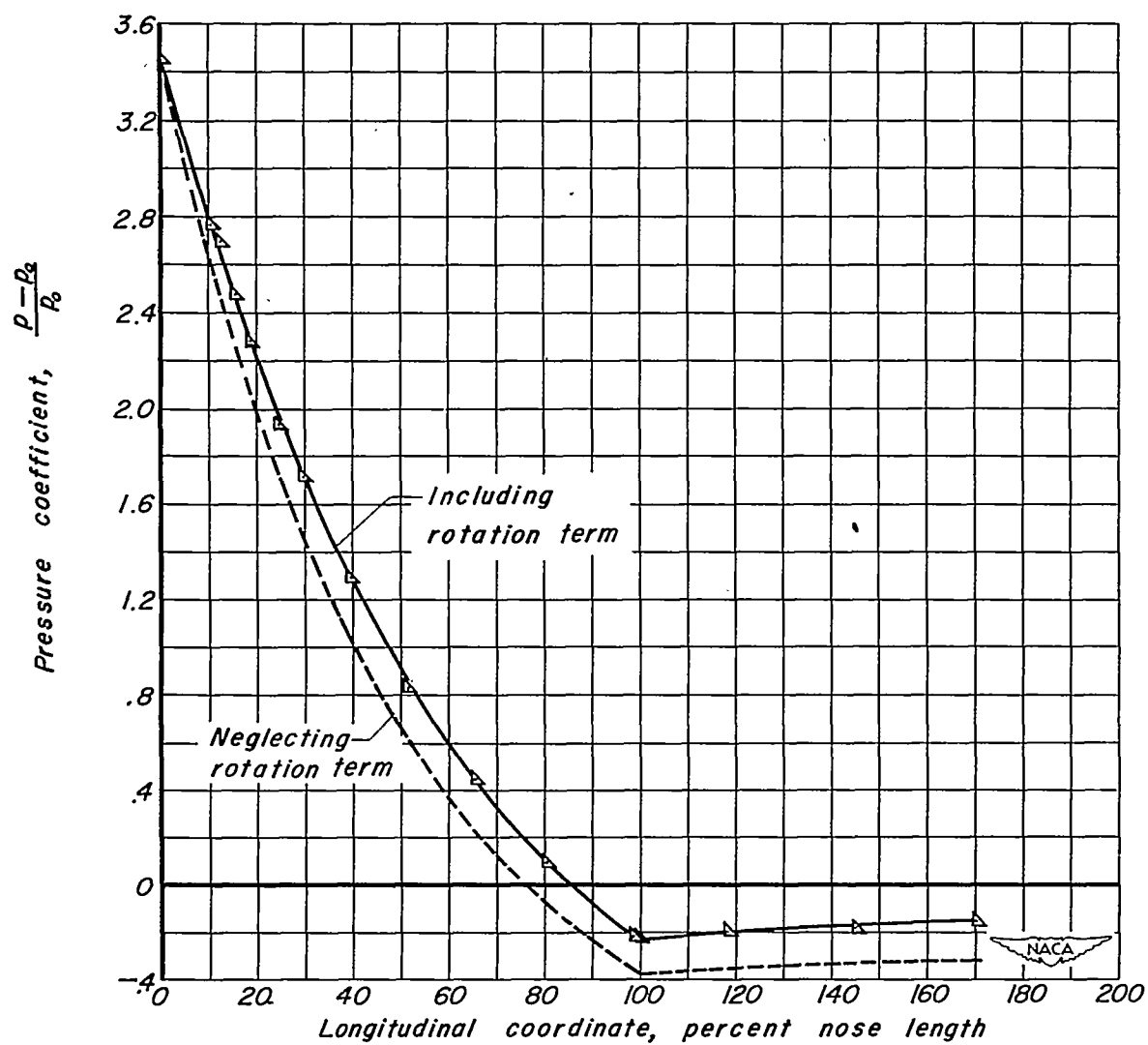
(b) $K = 1.0$

Figure 3.—Continued.



(c) $K = 1.5$, $\lambda/d = 4$, $M_\infty = 6$.

Figure 3.—Continued.

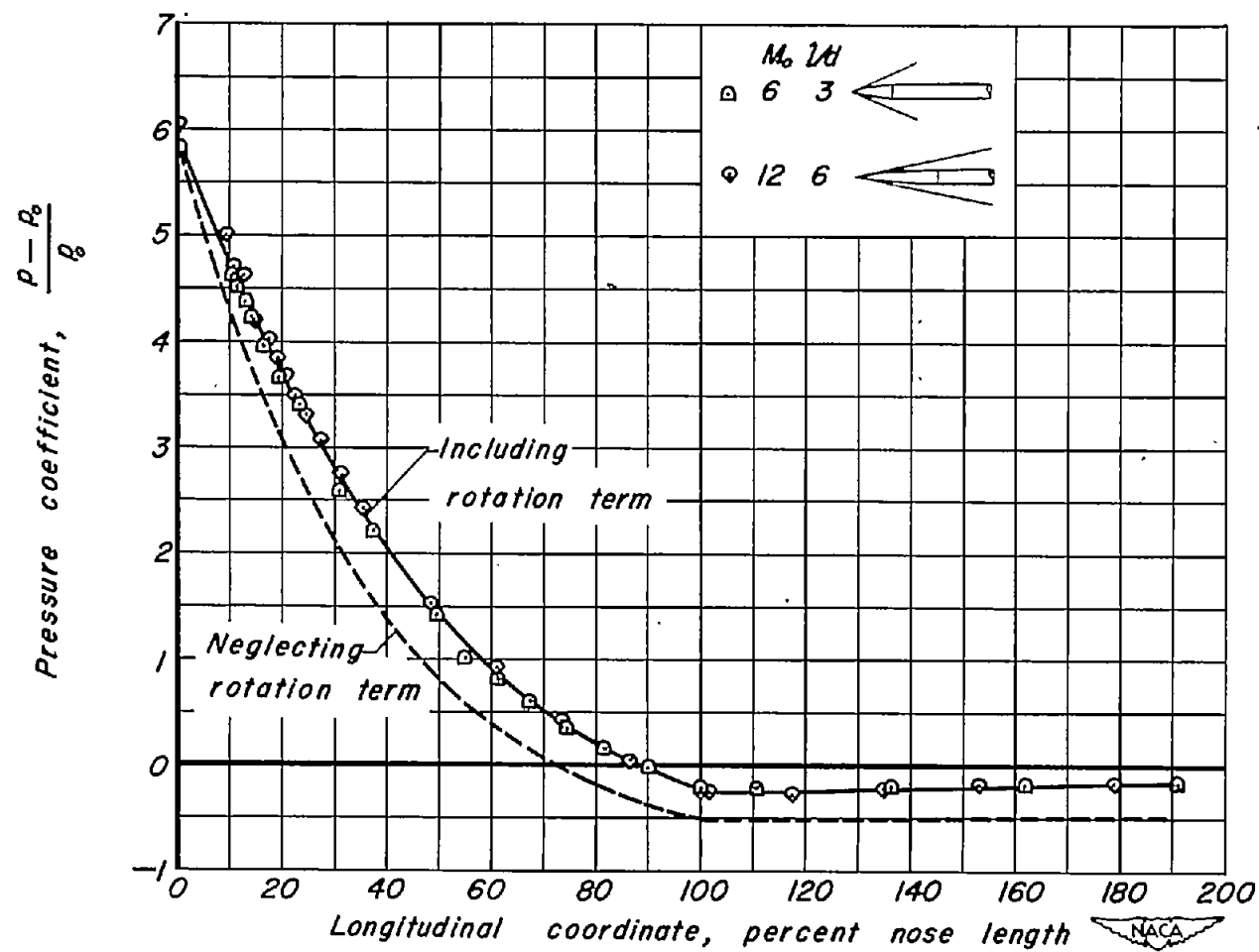
(d) $K = 2.0$

Figure 3.—Concluded.

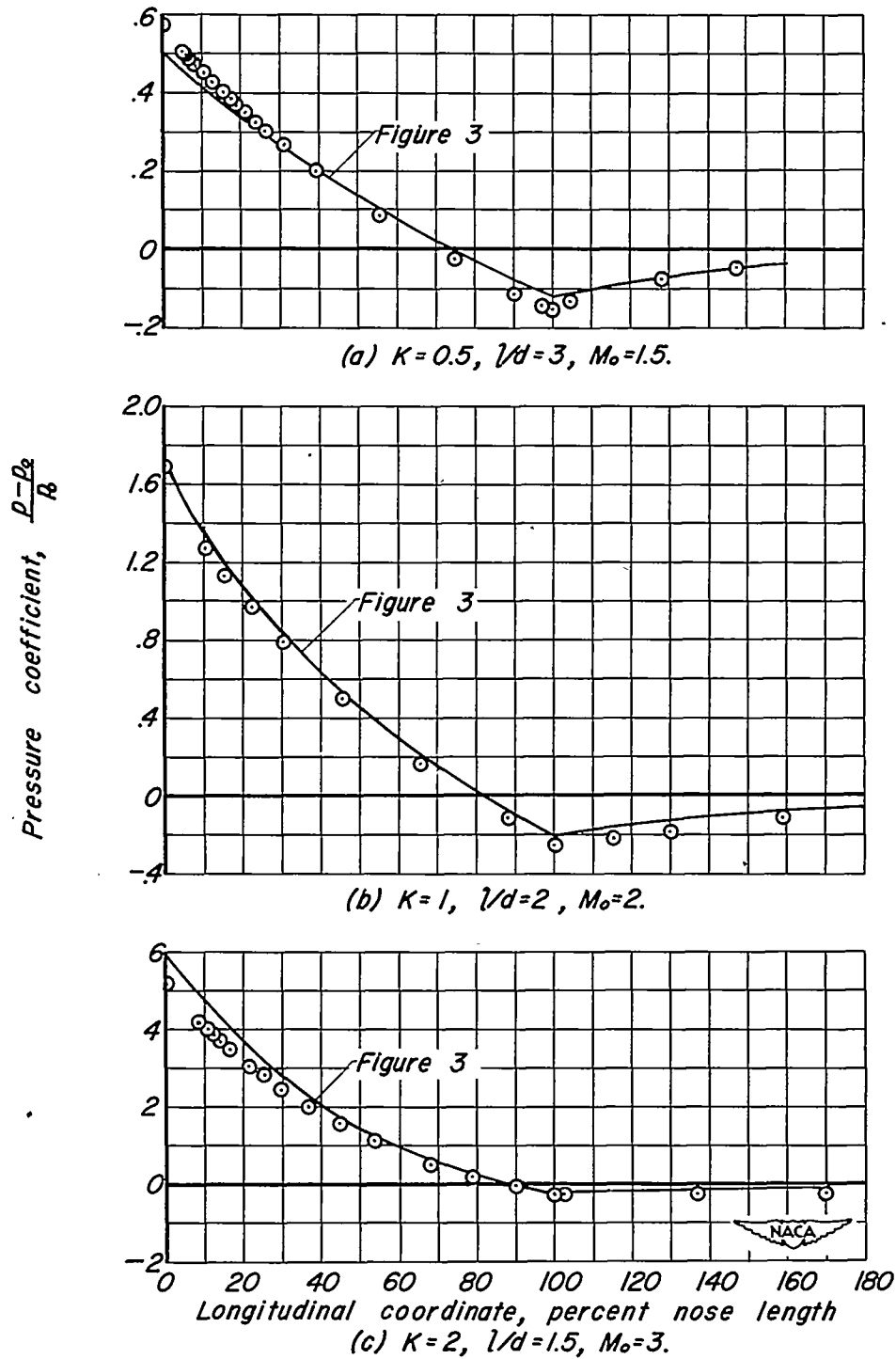


Figure 4.—Solutions to check the lower limits of Mach number and fineness ratio for which the hypersonic similarity law applies.

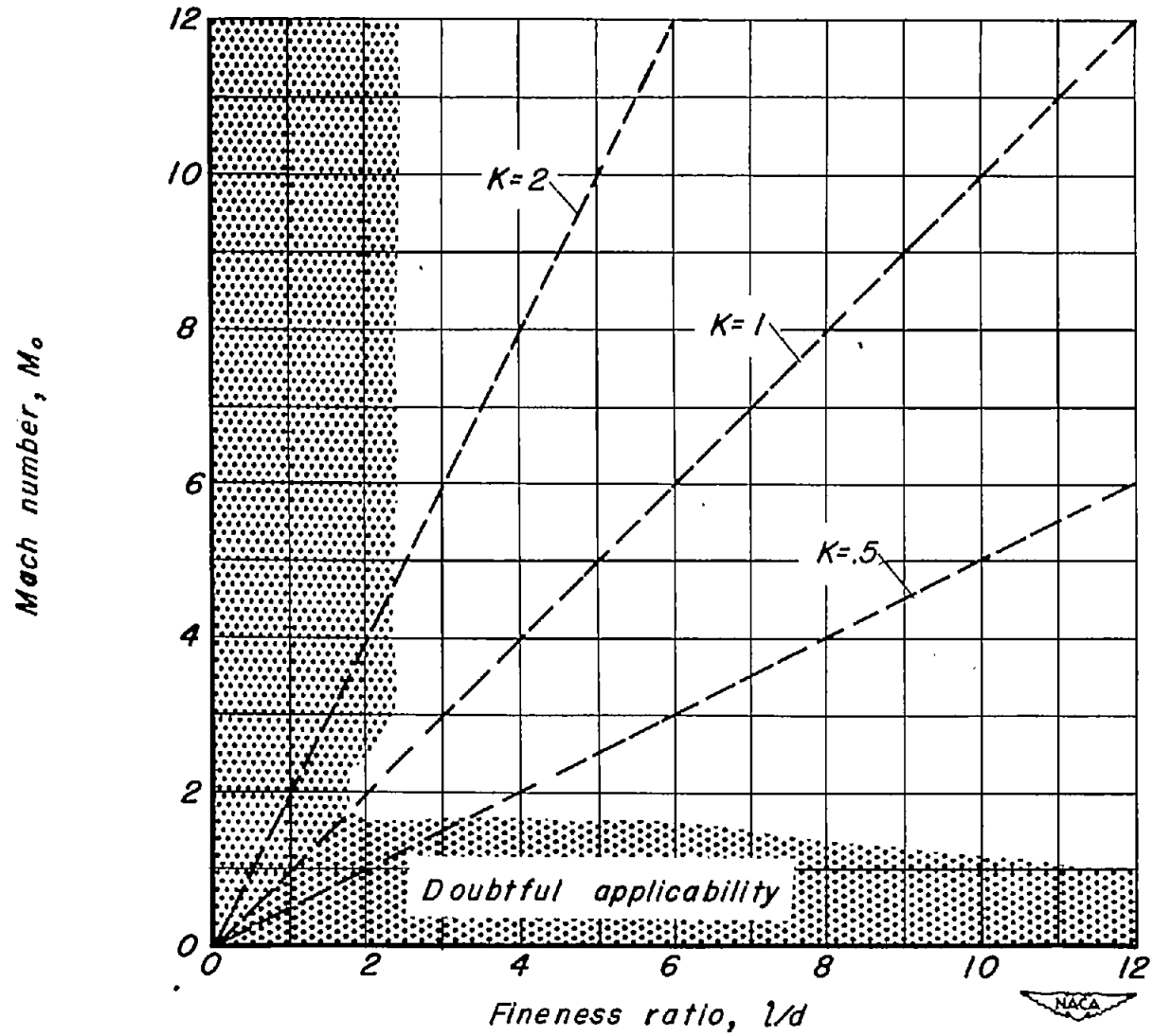
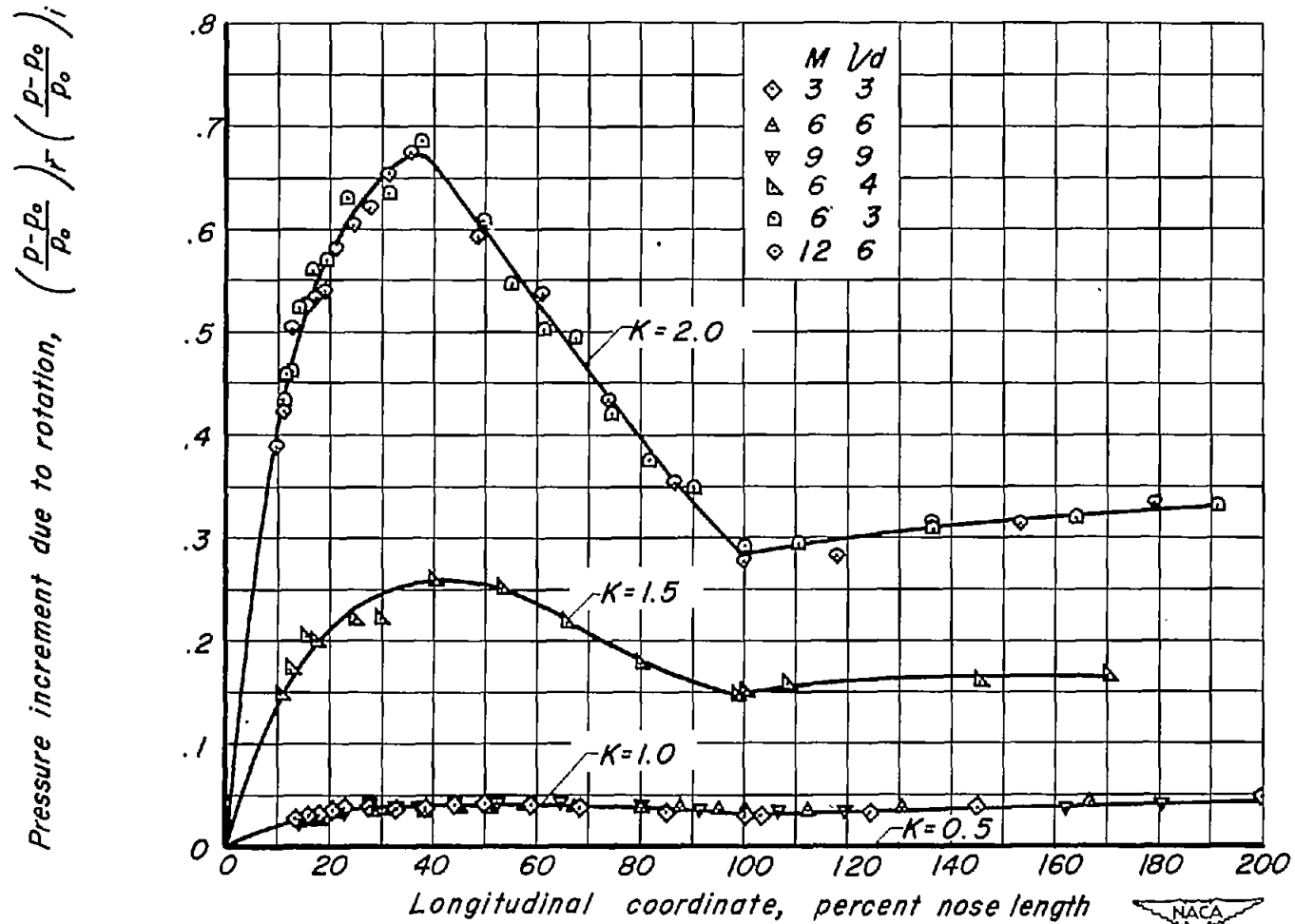


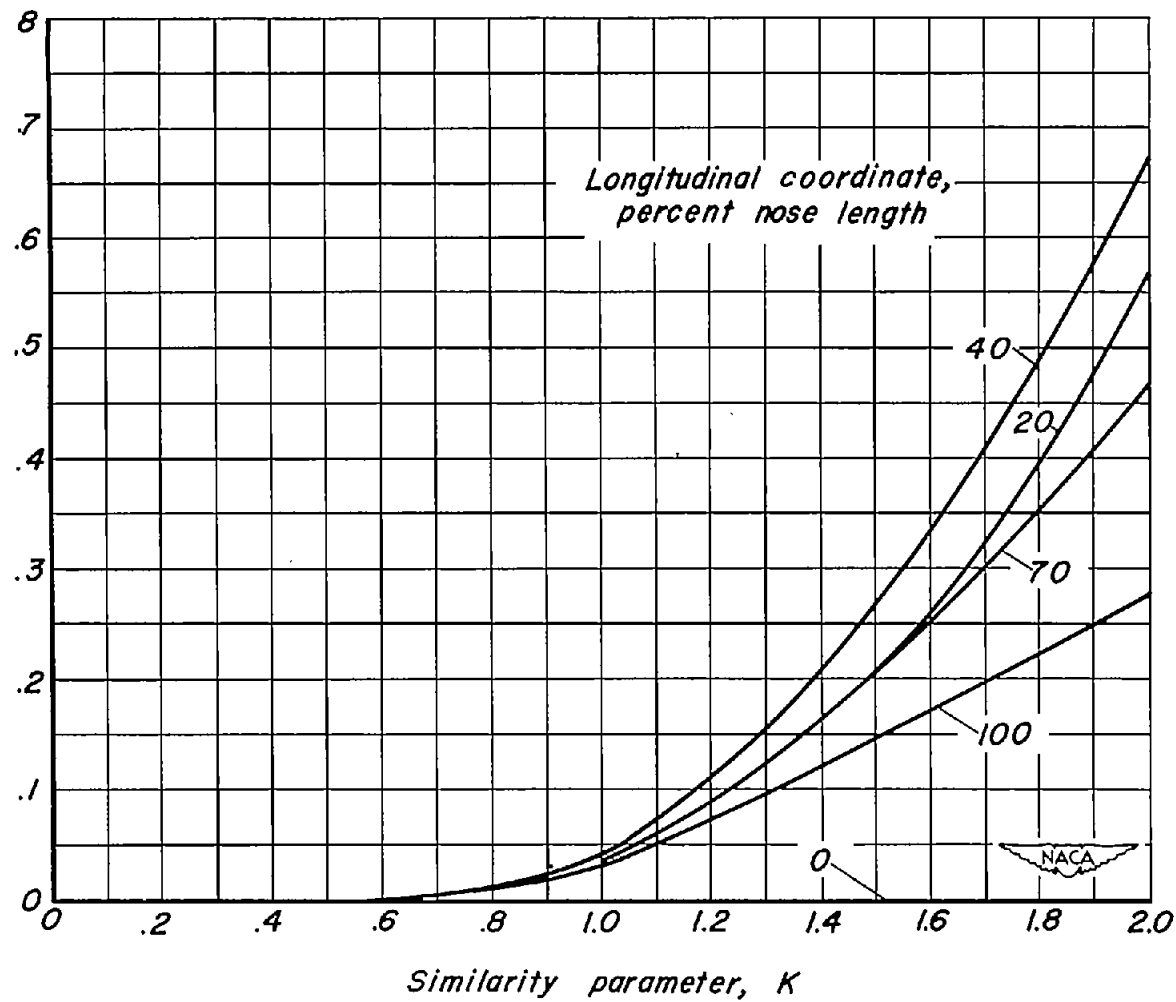
Figure 5.—Range of applicability of similarity law for ogives.



(a) Variation of pressure increment along body.

Figure 6.—Pressure increment along ogive cylinders due to rotation term in characteristics equation.

Pressure increment due to rotation, $\left(\frac{p-p_0}{p_0}\right)_r - \left(\frac{p-p_0}{p_0}\right)_i$



(b) Variation of pressure increment with K .

Figure 6.—Concluded.

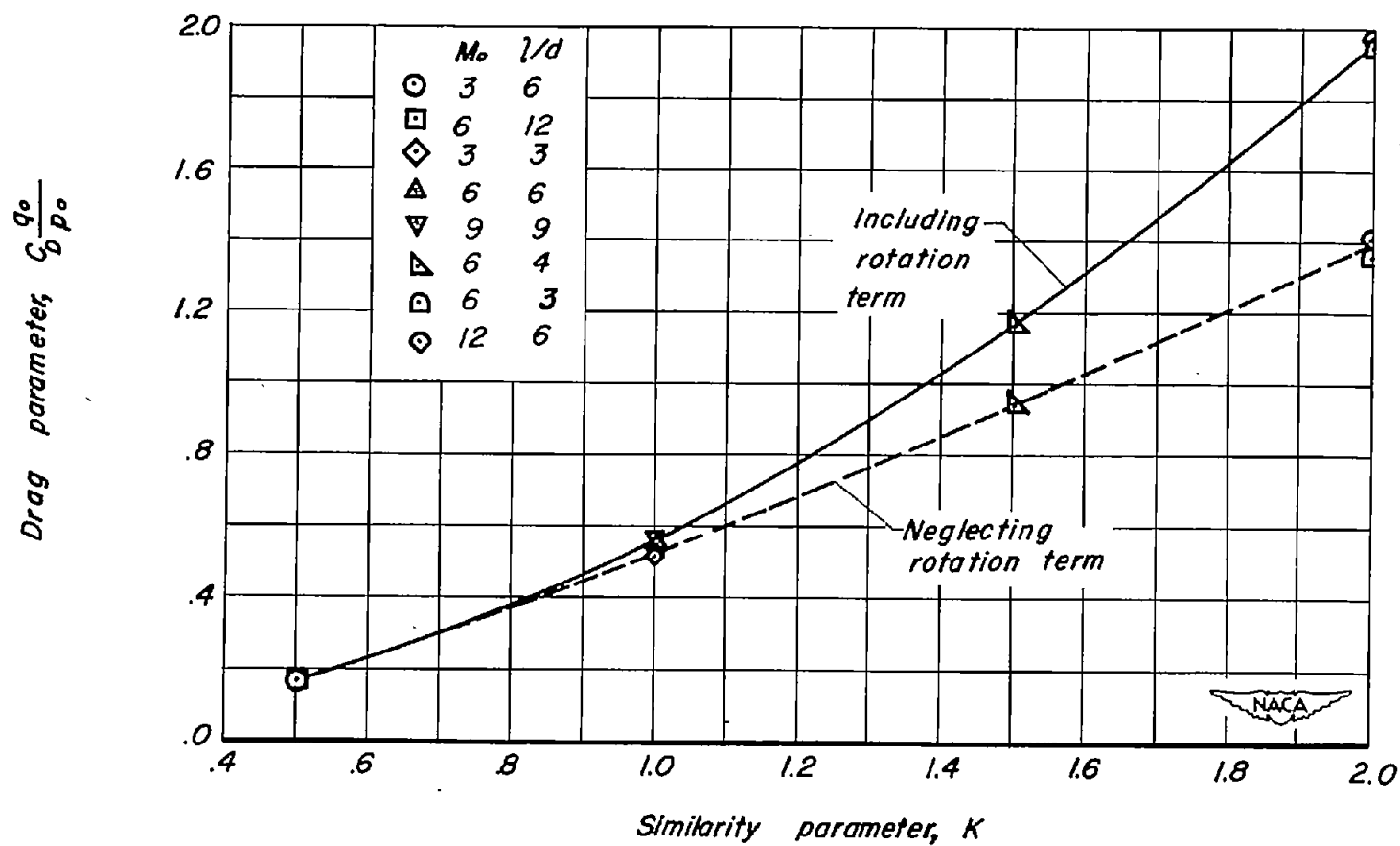
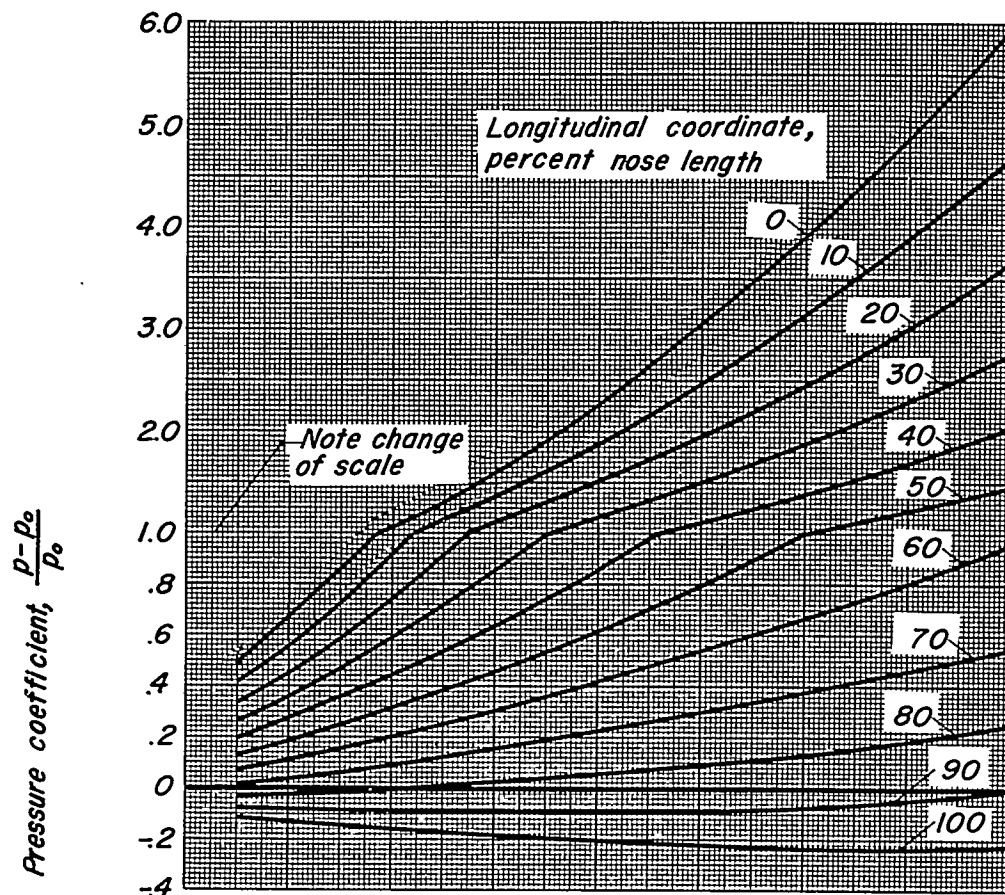
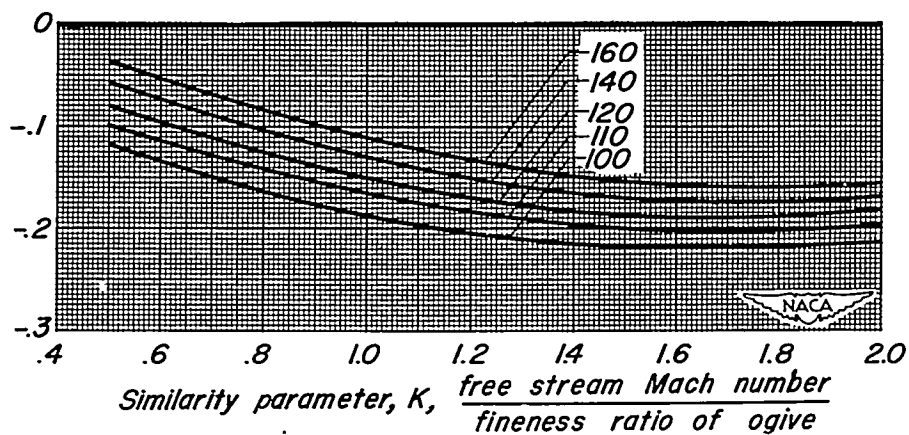


Figure 7.—Variation of drag parameter $C_D \frac{q_0}{\rho_0}$ with the similarity parameter K for ogives.



(a) Ogive



(b) Cylinder

Figure 8.—Variation of pressure coefficient with K for ogive cylinders including effects of rotational flow.

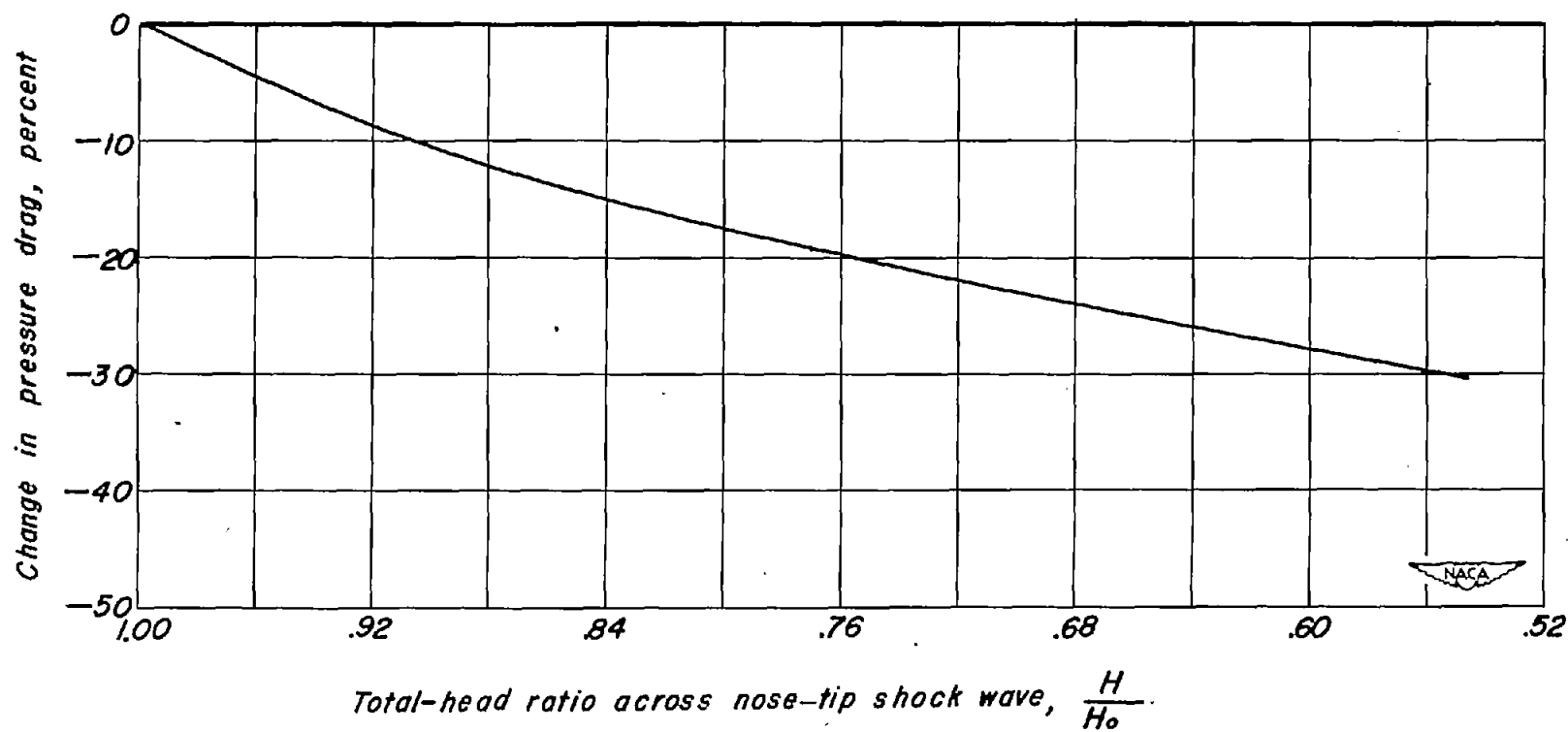
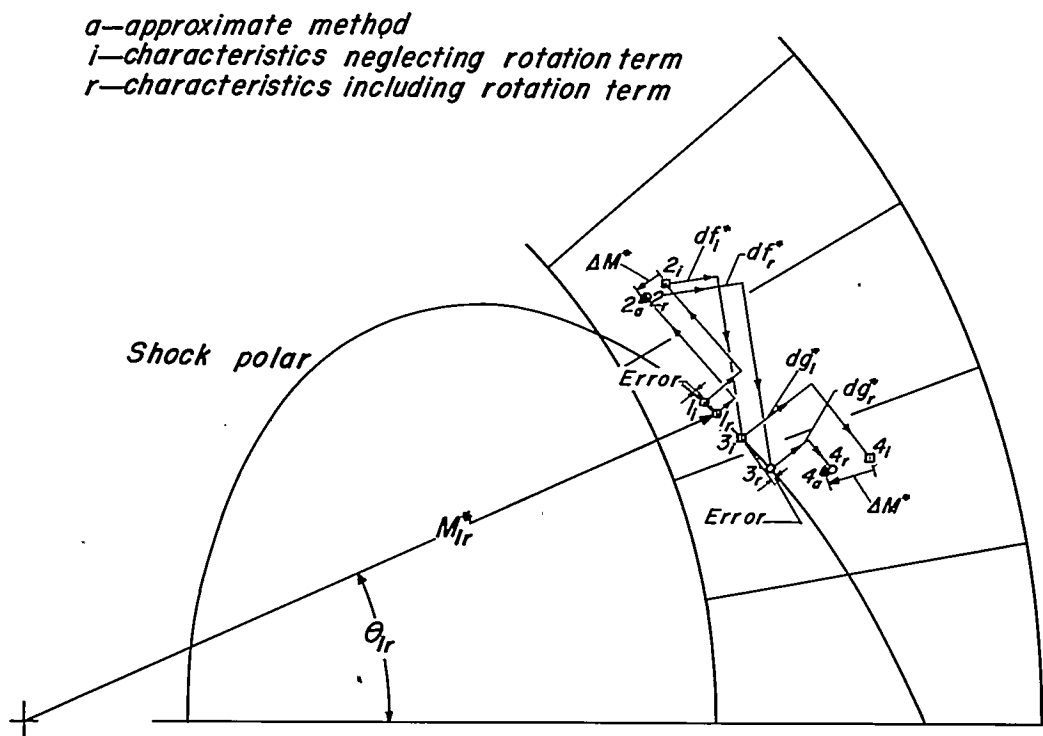
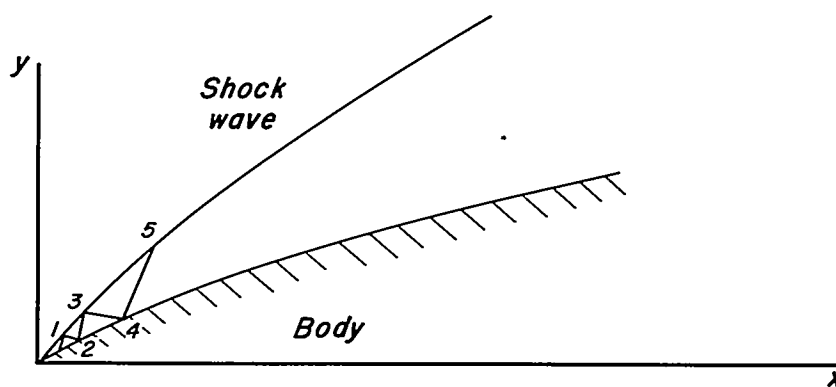


Figure 9.—Change in pressure drag of ogives due to neglect of rotation term in characteristics equation.



(a) Hodograph plane.



(b) Physical plane.



Figure 10.—Schematic diagram comparing the conventional and approximate method for including rotation.